Experiment 11

# Measurement of the mean lifetime of muons after absorption in aluminium

Advanced lab course for master students in elementary particle physics
RWTH Aachen University

2022

## Prerequisites

- Elementary particles: Classification, interactions, lifetime, energy loss
- Cosmic Rays: Sources, energies, air showers
- Photomultipliers and scintillators
- Method of delayed coincidence measurements
- Fitting curves to data using a computer

## Objectives

- Design and setup of a circuit for measurements with delayed coincidence
- Measurement of the mean lifetime of muons in aluminium
- Determination of the mean lifetime of free muons

# Contents

# 1 Cosmic radiation

## 1.1 Primary component of the cosmic radiation

The cosmic radiation registered at the surface of Earth consists primarily of secondary particles which are produced by means of interactions with atoms in the atmosphere. The content of this radiation does not coincide with the composition of the primary component of the cosmic radiation which reaches Earth from outer space. By means of measurements outside of the atmosphere (above 60 km height), the composition of the low energetic part of the primary component of the cosmic radiation has been determined (Tab. 1). It consists mainly of protons and some $\alpha$ particles. Heavy nuclei ($Z > 2$) are rare. The highest atomic number which has been detected in cosmic radiation yet amounts to about $Z = 100$.

| Percentage | Particle |
|---:|---|
| 92 % | protons |
| 6 % | $\alpha$ particles |
| 1.0 % | electrons |
| 0.9 % | heavy nuclei |
| 0.1 % | photons |
| few | positrons, anti-protons |

Table 1: Composition of the primary cosmic radiation.

The energies of cosmic radiation ranges from $10^7$ to $10^{20}$ eV. The highest energy of $3.2 \cdot 10^{20}$ eV has been observed with the Fly's-Eye telescope in Utah (USA). The occurance of cosmic radiation decreases strongly with its energy. For energies at about $10^{10}$ eV one particle per square meter and second reaches Earth. At energies of $10^{16}$ eV it decreases to one particle per square meter and year. At the highest energies of $10^{20}$ eV only one particle per square kilometer and century reaches Earth. The distribution of the particle flux with the energy of the particles, also referred to as the cosmic radiation spectrum is shown in Fig. 1.

As a consequence of the steeply falling energy spectrum, direct measurements of cosmic radiation is only possible up to an energy of about $10^{12}$ eV. Above Earth's atmosphere, the surfaces of detectors which can be operated on satellites and balloons are too small. Cosmic radiation with energies beyond $10^{12}$ eV can only be detected indirectly in measuring the secondary particles of their extended air showers.

Extended air showers can be studied in measuring them by means of an array of particle detectors on the ground or in measuring UV light produced by secondary particles crossing the atmosphere. The Pierre-Auger observatory, which is the biggest observatory for the detection of cosmic radiation, combines both methods.

The production mechanism of the cosmic radiation could not be clarified unambiguously yet. Common models assume that processes in the universe, releasing larger amounts of energy are responsible for the production of cosmic radiation. The sun is the main source for the lower part of the energy spectrum. Possible sources for the middle part of the energy spectrum are pulsars and supernovae explosions in our galaxy and their remainders. For the highest energies, active galactic nuclei (AGN) with black holes in their center, releasing a huge amount of energy, are assumed to be responsible.

## 1.2 Influence of the primary component

The sun wind consists mainly of low energetic protons and causes the low energetic cosmic radiation. Its influence reaches far beyond our solar system. It is responsible for variations in the intensity of the cosmic radiation which reaches Earth. The penetration of the cosmic radiation into the solar system depends on its strength. In neighborhood of Earth, outside of the atmosphere, Earth's magnetic field influences the cosmic radiation, too. Charged particles (in particular light ones like the electron) are partly reflected very strongly, causing them not to reach Earth's surface anymore. In this way, Earth's magnetic field causes the Van-Allen radiation belt in which electrons and protons of the cosmic radiation are forced onto circular orbits. The second effect of Earth's magnetic field is the decrease of the cosmic particle flux toward the equator. The measurements of the flux are so precise today that the variation of the earth's magnetic field can be deduced from it.

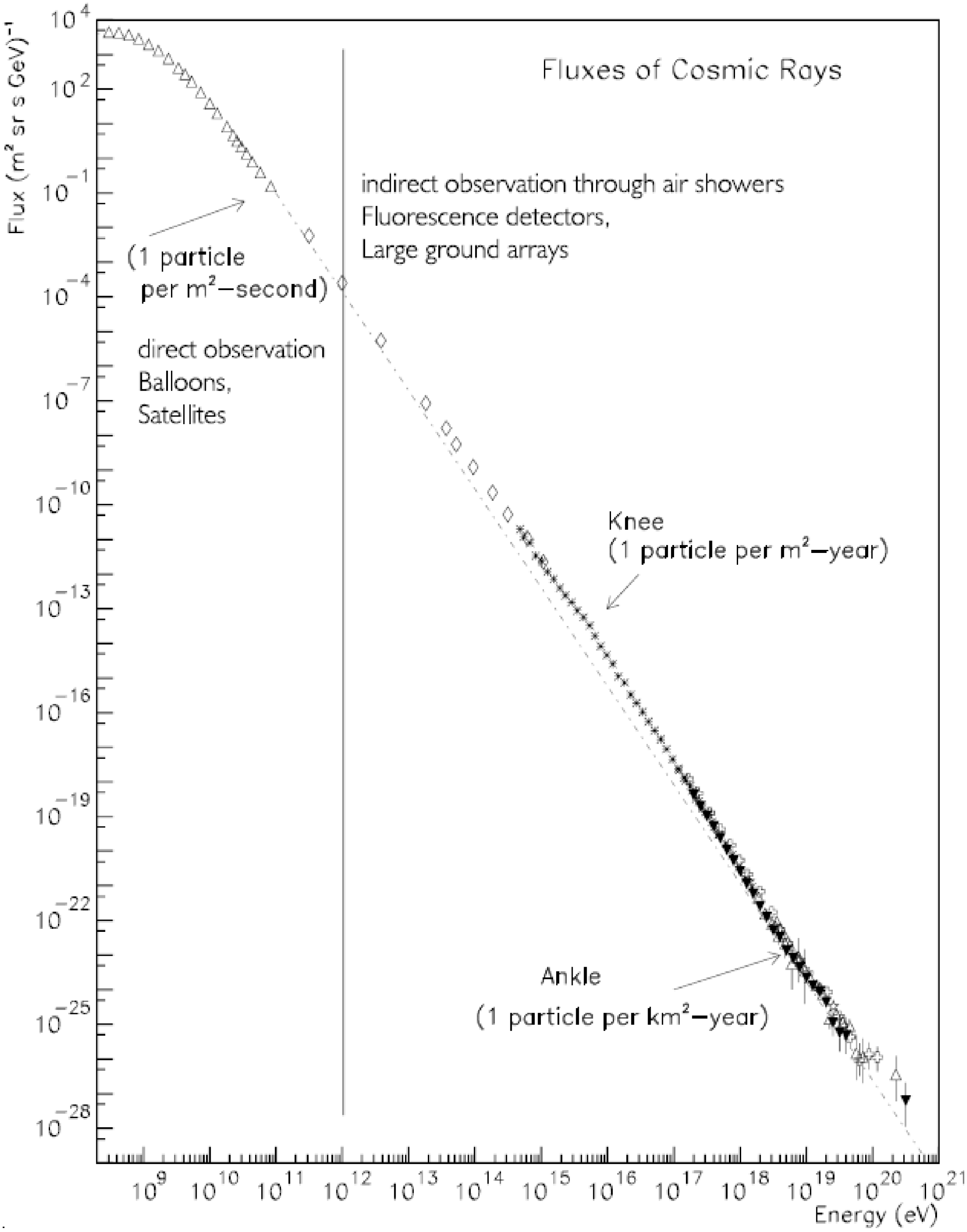


Figure 1: Energy spectrum of the cosmic radiation above the earth's atmosphere.

In direction measurements with coincidence counters it turns out that the rate of incident particles changes from east to west. The cause is the Lorentz force $\vec{F}_L = e(\vec{v} \times \vec{B}_{\mathrm{earth}})$, which bends the charged particles differently depending on their charge sign. This asymmetry in the particle rate shows that the majority of the particles in the cosmic radiation is charged positively (compare Tab. 1). The charged particles are not only influenced by Earth's magnetic field, but also by magnetic fields in and between the galaxies. Therefore, they are already deflected on the path to Earth, which makes it difficult to determine the direction of the particle origin.

When the particles enter Earth's atmosphere they are mainly influenced by interactions with atoms. Pressure and temperature also affect the particle rates measured at the ground. Since the majority of cosmic radiation consists of protons, their interactions in the atmosphere are discussed in more detail now. The primary protons can either collide with an electron or with a nucleus of an air molecule. Giving the height in units of mass occupancy (product of path length and density) the first collision takes place in average after $80\,\mathrm{g/cm^2}$. With the mass occupation of the whole atmosphere of $1000\,\mathrm{g/cm^2}$ (which is responsible for the pressure of $10^5$ Pa at Earth's surface) several collisions take place. The collisions with electrons cause ionization of the air while the protons loose energy according to the Bethe-Bloch formula. The electrons removed from the air molecules can in turn ionize further nuclei.

Proton collisions with the nuclei of air molecules produce (among others) short-lived particles (pions and kaons):

$$\mathrm{p} + \mathrm{nucleus} \rightarrow \pi^+, \pi^-, \pi^0, \mathrm{K}^+, \mathrm{K}^-, \mathrm{K}^0, \mathrm{p}, \mathrm{n}.$$

The secondary particles decay after relatively short time intervals (average lifetime: $\tau(\pi^\pm) = 26\,\mathrm{ns}$, $\tau(\mathrm{K}^\pm) = 12\,\mathrm{ns}$) into muons and neutrinos:

$$\begin{array}{ccl} \mathrm{K}^+ & \rightarrow & \mu^+ + \nu_\mu \\ \mathrm{K}^- & \rightarrow & \mu^- + \bar{\nu}_\mu \\ \mathrm{K}^0 & \rightarrow & \pi^\pm + \mathrm{leptons} \\ \pi^+ & \rightarrow & \mu^+ + \nu_\mu \\ \pi^- & \rightarrow & \mu^- + \bar{\nu}_\mu \end{array}$$

with a branching ratio of 63,5 % for the kaon decays given above. The kaons can also decay in into $\pi^0 + \pi^\pm$ in 21,1 % of cases. The pions in turn also decay rapidly. The $\mathrm{K}^0$ decays most frequently into a charged pion and lepton or into two or three uncharged pions. The second decay channel has not been included in the list above since it does not contribute to the muon flux. The uncharged pion does not contribute to the muon flux since it decays almost exclusively into two photons.

**Question 1** Which distance of flight does a positive pion with a kinetic energy of 1 GeV in the laboratory rest frame cover before it decays in average?

The produced muons reach Earth's surface due to their relatively long lifetime and the relativistic time dilatation while they suffer only little interactions with the atmosphere. Their deceleration takes place almost exclusively through ionization losses as usual for charged particles.

The secondary particles of the primary cosmic radiation can be subdivided into several cascades (Fig. 2). One is the nucleon cascade which consists of protons and neutrons knocked out from nuclei. The second is the muon cascade which consists of the decay of charged pions and kaons. The third is the electromagnetic cascade which consists of photons and electrons. The photons convert to $\mathrm{e}^+\mathrm{e}^-$ pairs which in turn create Bremsstrahlung. Fig. 2 is to be understood schematically - the cascades are not separated spatially in nature.

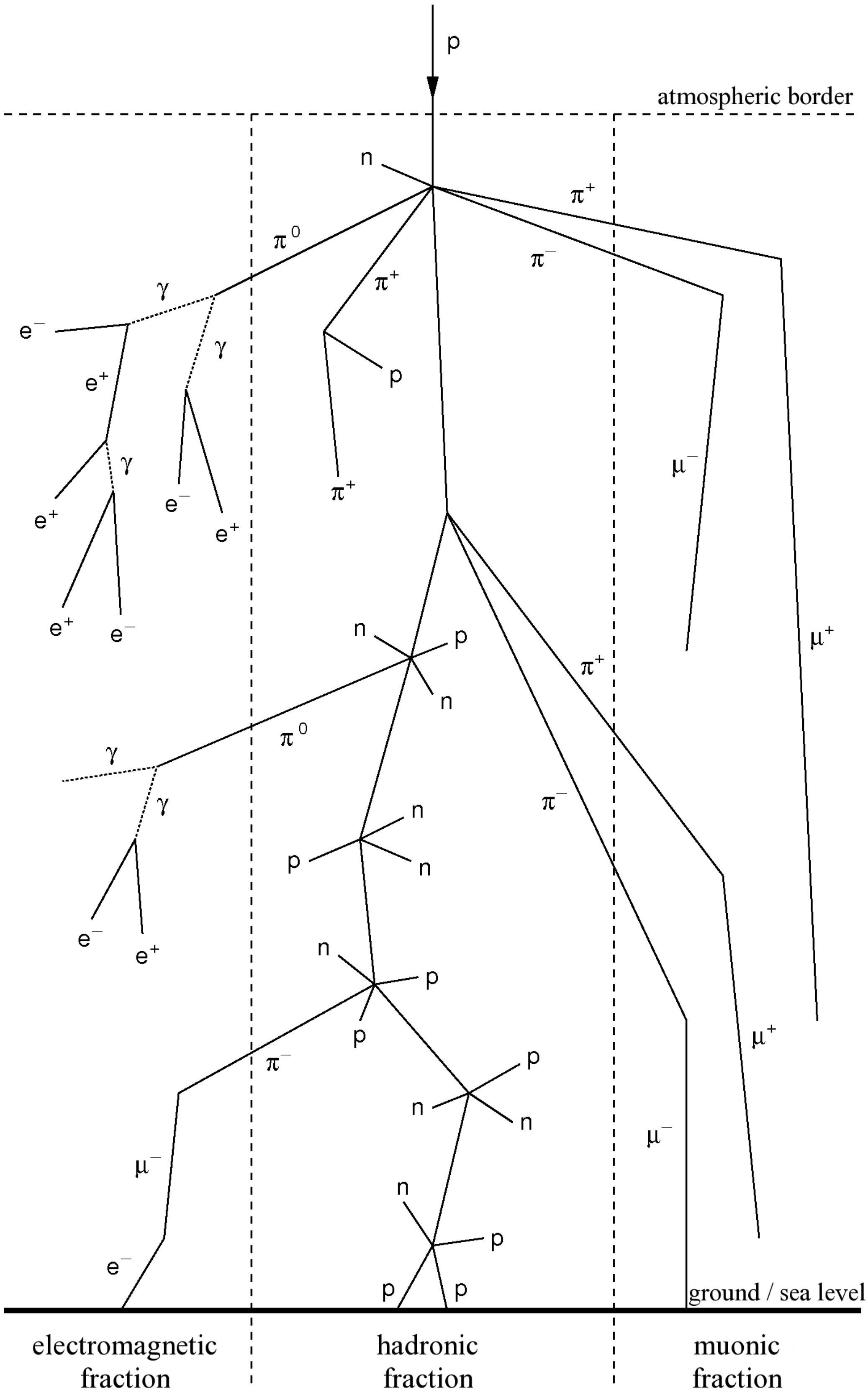


Figure 2: Development of cascades in the atmosphere.

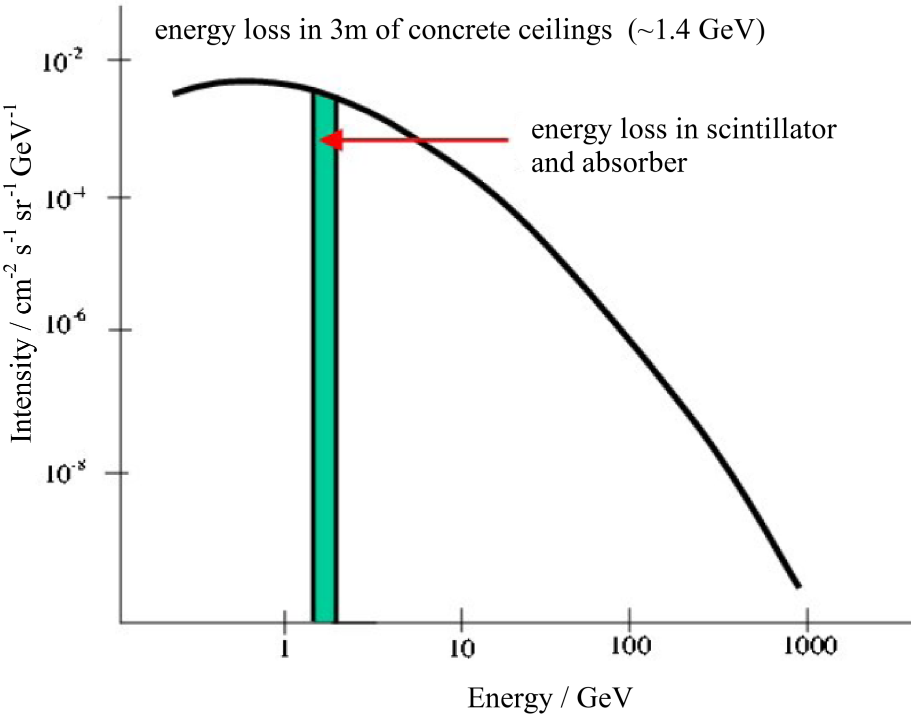


Figure 3: Energy spectrum of the muons at earth's surface.

## 1.3 Muon reactions

Free muons decay with a mean lifetime in the micro second range, the exact value is to be determined in this experiment. The decay products are electrons or positrons and two neutrinos (eq. (1) and (2)). The branching ratio for each decay channel amounts to 98,6 %. Furthermore, decays with an additional photon or an additional $e^+e^-$ pair are possible.

$$\mu^+ \rightarrow e^+ + \nu_e + \bar{\nu}_\mu \tag{1}$$
$$\mu^- \rightarrow e^- - \bar{\nu}_e + \nu_\mu \tag{2}$$

Figure 3 shows the energy spectrum of mouns reaching the ground. As already mentioned above, the muons are primarily decelerated by means of ionization. In the experimental setup used here only muons which get stopped in the 10 cm thick aluminium absorber are of interest. This means that only the low energetic part of the muon spectrum is exploited since the higher energetic muons fly through the target.

The low energetic muons are decelerated to thermal velocities in the target. In contrast to the $\mu^+$ the $\mu^-$ can then be captured in an atom, replacing an electron of the atomic shell:

$$\mu^- + \text{atom} \rightarrow \text{muonic atom} + e^-$$

In such a muonic atom the muon takes the role of an electron. But the muon can be distinguished from the other electrons in the shell such that the Pauli principle does not apply for the muon. Therefore the muon can assume the ground state in the shell. Since the capture happens in a highly excited state, photons are being emitted until the ground state is being reached. The time needed for these transitions is very small (about $10^{-14}$ s) compared to the lifetime of a free muon.

The probability of an electron to be located at the distance $r$ from the nucleus center is given by $|\psi(r)|^2\,4\pi r^2\,dr$ where the mere dependency of $r = |\vec{r}|$ is only valid for $l = 0$ (s-states). This probability has a maximum whose exact value has already been predicted by Niels Bohr with his semi-classical model. It can also be derived exactly in solving the Schrödinger equation of the quantum mechanical hydrogen problem. For the ground state the solution reads

$$a_0 = \frac{4\pi\varepsilon_0\hbar^2}{mZe^2}$$

This Bohr radius $a_0$ is smaller by the factor $m_{\mathrm{e}}/m_\mu \approx 1/207$ for the muon due to its larger mass compared to the electron. This means that the maximal probability density of a muon is much closer to the nucleus compared to an electron in the shell.

The probability density $\psi(r)$ of the s-states are different from zero at the location of the nucleus which provides the possibility for the muon to react via the weak interaction with the nucleus:

$$\mu^- + \mathrm{p} \rightarrow \nu_\mu + \mathrm{n} \tag{3}$$

With increasing atomic number, i.e. with increasing nucleus size, the probability for such a muon capture increases, too. In heavy nuclei the Bohr radius of muons is of the same size as the nucleus radius. Therefore, the probability density inside the nucleus is large enough for the muon to be captured on an essentially shorter time scale compared to the free muon lifetime. The capture probability per time unit $\lambda_c$ (c: capture) is proportional to the probability density of the muon inside the volume of the nucleus. The exact capture probability is to be computed quantum mechanically and has been measured for many materials.

The total probability per time unit for a muon to disappear from a K-shell is $\lambda_- = \lambda_{\mathrm{free}} + \lambda_c$ where $\lambda_{\mathrm{free}}$ corresponds to the decay probability of the free muon and $\lambda_c$ to the capture probability of the muon in the K-shell. The mean lifetime $\tau_-$ for negative muons is then given by

$$\tau_- = \frac{1}{\lambda_-} = \frac{1}{\lambda_{\mathrm{free}} + \lambda_c}.$$

For positive muons, no capture decay channel exists. Therefore their decay probability $\lambda_+$ is exclusively given by $\lambda_{\mathrm{free}}$ and the lifetime of positive muons in matter is larger compared to negative ones. The detector used in this experiment is not able to distinguish between negative and positive muons. Therefore a combined decay distribution is obtained.

| T [MeV] | 10 | 20 | 30 | 40 | 50 | 60 | 70 | 80 |
|---|---|---|---|---|---|---|---|---|
| $k_\mu$ $[MeV \frac{cm^2}{g}]$ | 7.91 | 4.82 | 3.73 | 3.19 | 2.86 | 2.65 | 2.49 | 2.38 |
| T [MeV] | 90 | 100 | 200 | 300 | 400 | 500 | 600 | 700 |
| $k_\mu$ $[MeV \frac{cm^2}{g}]$ | 2.30 | 2.23 | 1.99 | 1.96 | 1.96 | 1.98 | 2.00 | 2.02 |
| T [MeV] | 800 | 900 | 1000 | 2000 | 4000 | 6000 | 10000 | |
| $k_\mu$ $[MeV \frac{cm^2}{g}]$ | 2.03 | 2.05 | 2.07 | 2.17 | 2.28 | 2.34 | 2.40 | |

Table 2: Average energy loss $k_\mu = \frac{1}{\rho}\frac{dE}{dx}$ of muons via ionisation in a material of density $\rho$ at a kinetic energy T in MeV.

# 2 Setup

## 2.1 Detector

Muons and their decay products are detected in two plastic scintillators each with an area of $120 \times 120\,\text{cm}^2$ and a thickness of 5 cm. Between both scintillators, an aluminium absorber of the same area and 10 cm thickness is placed. The light from the scintillators is directed towards photomultipliers using aluminum cones which are coated with an aluminised mylar film on the inside. Two photomultipliers are observing the scintillator from each of the far ends of the cones, PM1 and PM2 at the upper end and PM3 and PM4 at the lower end.

Incoming muons have to produce a start signal when creating light in the upper scintillator. The stop signal has to come from the lower scintillator created by the decay products of stopped muons. The maximum yield of start signals is expected under an inclination of 0°with respect to the vertical axis. For larger angles, one finds the distribution depicted in figure 4. The angle $\theta$ is the angle between the telescope[1] and the zenith ($\theta$=0°).

## 2.2 Data Acquisition

The signals of all photomultiplier tubes (PMT) (upper scintillator: PM1 and PM2, lower scintillator: PM3 and PM4) should first be processed by discriminators. Once a signal falls below a certain threshold, a logic signal of adjustable duration is generated. The thresholds have to be set in a way that noise from the electronics and from the PMTs is rejected while pulses originating from real muon hits are accepted (cf. 5). After this stage, a coincidence circuit has to be set up which processes the signals from the upper and lower PMTs and allows the measurement of their time difference.

The time-to-amplitude converter (TAC) is the central component of this circuit. The measurement of the decay time is done by first producing a start signal when a muon passes the upper scintillator and subsequently a stop signal when the electron (or positron) from the muon decay enters the lower scintillator. Out of the time difference between those signals, the TAC generates an output signal with a corresponding pulse height. This signal is fed into the multi-channel analyser (MCA) and displayed on the PC. Thus, the pulse-height spectrum measured by the MCA corresponds to the time spectrum of the muon decays. A a time window has to be selected at the TAC, which determines the period following a valid start signal during which the TAC accepts a stop signal. If no stop signal arrives within this period (the electron/positron may not have reached the scintillator) the TAC discards the start signal and waits for the next one. Once the TAC was triggered by a start signal, it ignores further start signals until the time limit for stop signals is reached. In order to eliminate unwanted events before they can trigger the TAC, a logic circuit has to be set up. Think about which kinds of events the detector can produce and what logic is needed to determine whether an event from the detector is useful or not. The goal is to select as many useful events as possible while rejecting most of the unwanted events at the same time.

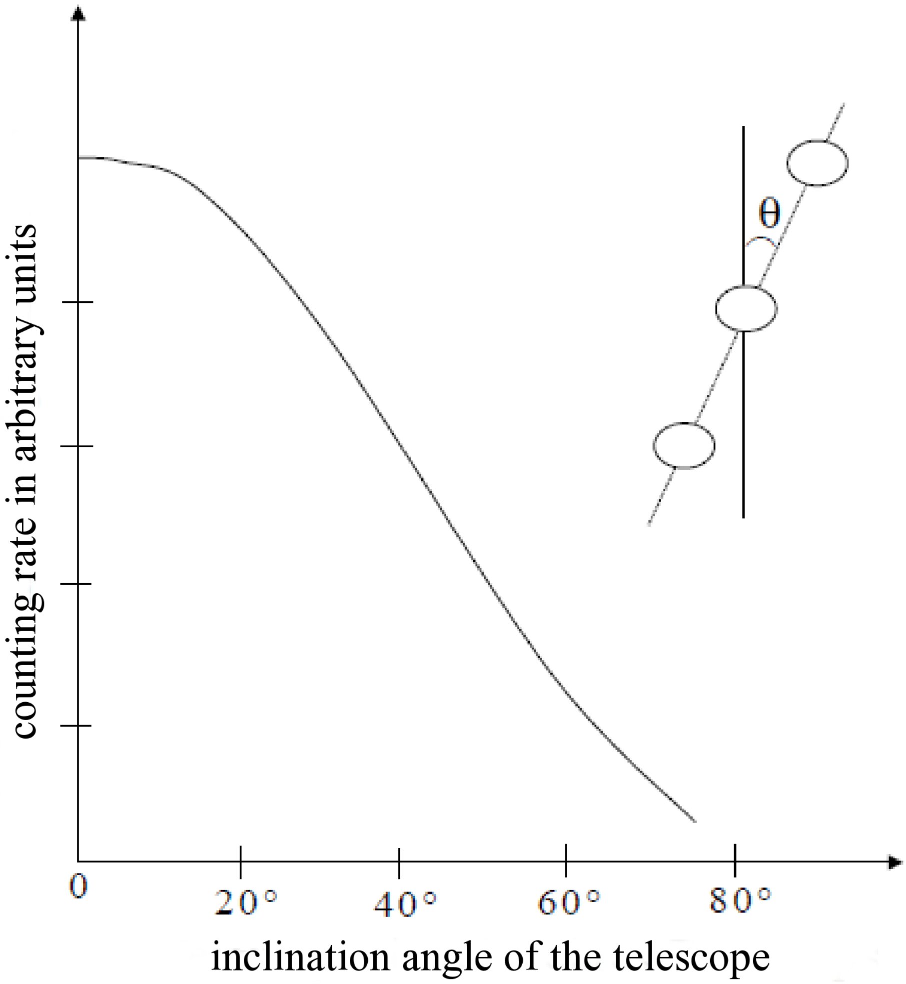


Figure 4: Angular distribution of the incoming muons.

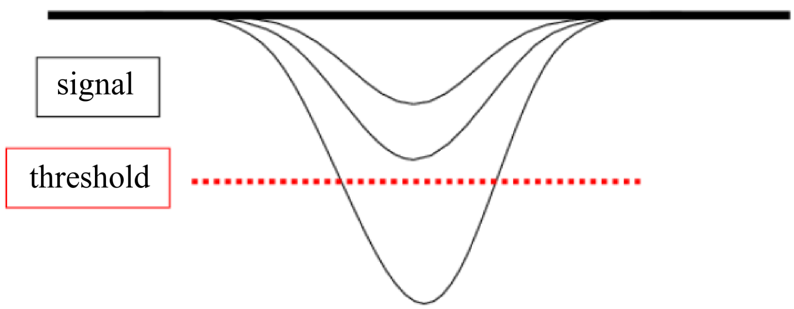


Figure 5: Setting of the discriminator threshold.

## 2.3 Questions and Problems

**Question 1** Are the decay products in the lower scintillator the only cause of a stop signal?

**Problem 2** Determine the maximum kinetic energy a muon may have when entering the upper scintillator in order to be stopped at the lower edge of the aluminium absorber. Use the energy dependent energy loss via ionisation given in table 2. The density $\rho$ of the scintillator material is 0.91 $\frac{g}{cm^3}$, the one of aluminium is 2.72 $\frac{\mathrm{g}}{\mathrm{cm}^3}$.

**Question 2** Does the measured lifetime depend on the distance the muons have covered in the atmosphere?

**Question 3** What spectrum can finally be seen on the PC?

**Question 4** What is the optimal choice for the maximum time window of the TAC in order not to lose too many valid events?

**Problem 3** What is the approximate time difference between start and stop signal caused by a 1 GeV muon passing through the detector?

**Problem 4** Think of a logic circuit for each measurement before the preliminary discussion.

[1]the circles represent particle detectors, e.g. Geiger-Müller counters

# 3 Running the experiment

Before starting the experiment find out about the functioning of its components and the working principle of the setup. Power down the NIM crates before inserting any modules. The next step is to power up the photomultipliers, the starting point is to be set to a voltage of 1.3 V (the maximum allowed voltage is 1.4 V, an operation below 0.5 V is not useful).

Make yourself familiar with the oscilloscope, it will be needed to check the signals and their propagation through the setup. Use the manuals of the NIM modules to understand their mode of operation.

## 3.1 Determination of the operating points of the photomultiplier tubes

In a first step, the operating points of the photomultiplier tubes have to be determined. The aim is to achieve an optimal signal efficiency while keeping the noise rate low. For this purpose, size and shape of the signals have to be looked at first. Then, a circuit has to be designed which allows to determine the voltage dependence of a 3-fold coincidence of the other photomultipliers and the rate of the 4-fold coincidence of all photomultipliers. Those rates can then be used to determine the efficiency of the photomultiplier under study in relation to the remaining photomultipliers.

This method is then applied successively to all photomultipliers: Firstly, the voltages of PM2, PM3 and PM4 are set to 1.3 V. The efficiency of PM1 is then measured in the voltage range from 0.5 V to 1.4 V and the point of optimal efficiency is determined. After setting PM1 to the corresponding voltage, the procedure is repeated for PM2, PM3 and then PM4, respectively. The whole cycle is repeated once or twice until the results are stable. All photomultipliers should now be operated at their optimal voltage and those must not be changed anymore for the rest of the experiment.

**Question 6** How does one choose the optimal operating point of a photomultiplier?

## 3.2 Calibration of the time measurement

When the operating points are determined, the complete measurement setup is assembled. Once this has been done, a time calibration has to be performed in order to establish the proper relation between the time difference of start and stop signal and the channel number given by the MCA. This can be achieved by using one photomultiplier as a signal source and by distributing its signals such that they trigger a start signal and a delayed stop signal. The delay has to be varied in a way that the relation between time difference and channel number can be examined over the full range of the MCA. This relation should be strictly linear, any significant deviation has to be checked.

## 3.3 Data collection

After calibrating the time measurement restore the actual measurement circuit and start the data acquisition on the PC. Then wait for half an hour and check the proper functioning of the setup with the collected data.

Due to the low rate (O(Hz)) data should be collected for a few days and can be retrieved immediately before the next group starts.

# 4 Evaluation of the experiment

Firstly, discuss the determination of the operating points of the PMTs and their result, then the time calibration of the MCA.

When evaluating the data one has to consider that the decay curve $I(t)$ consists of (at least) two components and a background $c_3$:

$$I(t) = c_1\, e^{-\lambda_- t} + c_2\, e^{-\lambda_+ t} + c_3 \tag{4}$$

The first term describes the decay of the negative muons, the second one that of the positive muons, respectively. The constant $c_3$ represents the background. The decay constant $\lambda_+$ corresponds to the one of free muons ($\lambda_{\text{free}}$) whereas the decay constant $\lambda_-$ is a combination of $\lambda_{\text{free}}$ and $\lambda_c$. Since in cosmic rays positive muons are only a little more frequent (less than 30%, cf. literature) than negative muons, the factors $c_1$ and $c_2$ should be approximately equal.

Due to its low atomic number ($Z_{\text{Al}} = 13$) the absorber is suitable for measuring both, the fast and the slow decay constants. When evaluating the MCA's data one has to take care to combine a certain number of channels in order to reduce fluctuations in the measurement. Before doing this one should roughly identify the following regions in the spectrum of the MCA:

- Range 1: the decay of the negative muons,
- Range 2: the decay of the positive muons,
- Range 3: the background

Thus, for the correct evaluation of the total decay curve one has to first make a guess where those regions are and then proceed with the analysis. Interpret the MCA's pulse height spectrum and explain the choice of the regions given above as well as the rebinning of MCA channels. The evaluation should then proceed in the following way: First determine the background level from the third range and subtract it from the spectrum. Propagate the errors and plot the resulting spectrum on a semi-logarithmic scale. At this stage one should also check whether the error of the time calibration is of importance here or if it can be neglected. Now determine the decay constant $\lambda_+$ of positive muons from a linear fit in the second range. Then extrapolate this to the first range and subtract this contribution. Then proceed in the same manner to determine the fast decay constant $\lambda_-$.

In addition one should perform various fits to the spectrum in linear representation: Including background, after background subtraction and after subtracting the fraction of long-lived muons ($\mu^+$). Present all values (including errors) for $\lambda_-$,$\lambda_+$,$\lambda_c$ and $\lambda_{\text{free}}$ in a table and compare them among each other. Also discuss their values and compare them to the corresponding results from literature.

All problems and questions from the manual have to be included in the evaluation.

## 5 Literature

Useful literature for preparation and evaluation:

## References

[1] C. Grupen (Ed.): Astroteilchenphysik, Vieweg-Verlag 2000

[2] Bruno Rossi: Cosmic Rays (1964)

[3] Otto Claus Allkofer: Introduction to Cosmic Radiation (1975), Bl 202

[4] J. G. Wilson: Cosmic Rays (1976), Bl 215

[5] Particle Data Booklet

[6] Particle Data Group Homepage: http://pdg.lbl.gov/

[7] J. M. Baxendale, C. J. Hume and M. G. Thompson: Precise measurement of the sea level muon charge ratio ( Journal of Physics G: Nuclear and Particle Physics 1 (1975) 781)

[8] J. Kremer et al.: Measurement of ground level muons at two geomagnetic locations (Physical Review Letters 83 (1999) 4241)

[9] T. Suzuki, D. F. Measdey: Total capture rates for negative muons (Physical Review C 35 (1987) 2212)

[10] D. F. Measdey: The nuclear physiscs of muon capture (Physics Reports 354 (2001) 243)